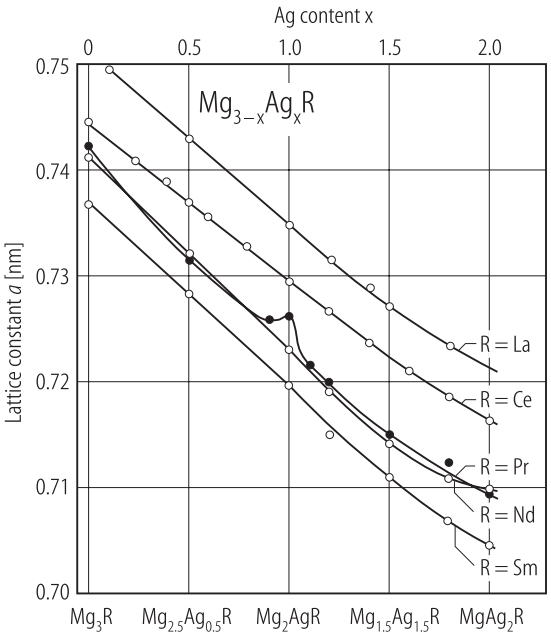

Fig. 34. Lattice constants of $Mg_{3-x}Ag_xR$ as a function of x [88B1].

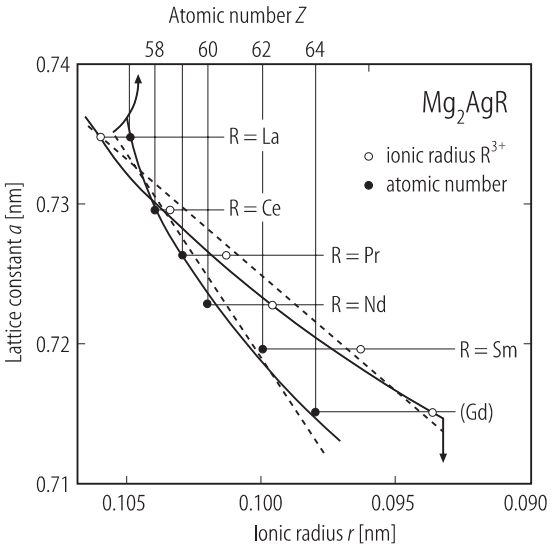

Fig. 35. Lattice constants of Mg_2AgR as a function of the atomic number Z and of the radius r (R^{3+}) respectively [88B1].

Pd–Y–Sn

The phase relations in the palladium-rich corner of the phase diagram have been extensively investigated. Five ternary phases were identified but only the Heusler β phase was found to be superconducting.

Table 8. A summary of the properties of selected alloys in the ternary phase diagram shown in Fig. 36 [85J3]. T_m: melting point, T_c: superconducting transition temperature, ρ: density.

Pd [at%]	Y [at%]	Sn [at%]	T_m [K]	Equilibrium composition at 1073 K	T_c [K]	Vickers microhardness [kgf mm^{-2}]	ρ [g cm^{-3}]
50	30	20	1413	β + Pd_5Y_4	3.65		
50	26	24		β	4	600	
50	25	25	1223	α + β	3.50		
50	25	25			5.5		
50	20	30	1233	α + β	5.20		
50	17	33	1233	α + β	5.20	560 + 575	
50	15.5	34.5	1228	α		550	9.0 ± 0.4
52	26	22	1748	β	3.75	582	8.7 ± 0.3
52	26	22			5.0		
52	24	24	1213	β + δ	5.5		
52.5	22.5	25	1213	β + ε + δ	3.2		
52.5	20	27.5	1143	β + γ + δ	4.6		
52.5	18.5	30	1153	α + β + γ	4.5		

Pd [at%]	Y [at%]	Sn [at%]	T_m [K]	Equilibrium composition at 1073 K	T_c [K]	Vickers microhardness [kgf mm^{-2}]	ρ [g cm^{-3}]
52.5	16	32.5	1153	$\alpha + \gamma$			
54	24	22	1698	β	5	570	
54	22	24	1233	$\beta + \varepsilon$	5.2		
54	17	29		γ		540	7.6 ± 0.1
55	23	22	1243	$\beta + Pd_3Y + \varepsilon$	4		
55	20	25	1233	$\beta + \varepsilon$	5.2		
55	17.5	27.5	1153	$\delta + \gamma + \varepsilon$			
55	15	30	1153	$\gamma + \varepsilon$			
56.5	17.5	26		$\beta + \varepsilon + \delta$			
57	14	29		$\delta + \varepsilon + Pd_3Sn_2$			
57.5	20	22.5	1233	$\beta, \varepsilon + Pd_3Y$	4.0		
57.5	17.5	25	1233	$\beta + \varepsilon + \delta$	4.4		
57.5	12.5	30	1158	$\gamma + Pd_3Sn_2$			
60	18	22	1233	$\beta + \varepsilon + Pd_3Y$	3.6		
60	15	25	1233	$\beta + \varepsilon$	4.4		
60	12.5	27.5	1233	$\delta + \gamma + \varepsilon$			
60	10	30	1223	$\gamma + \varepsilon + Pd_3Sn_2$			
62.5	12.5	25		$\beta + \varepsilon$	4.4		
67	17	16		$\beta + \varepsilon + Pd_3Y$			
69	5	26		$\varepsilon + Pd_3Sn$			
65	8	27		ε		525	9.2 ± 0.5

Table 9. *d* values and observed diffraction intensities of the γ, δ and ε phases (Fig. 36) [85J3]. w: weak, m: medium, s: strong, and vs: very strong intensity.

$Pd_{0.54}Y_{0.17}Sn_{0.29}$ (γ)		$Pd_{0.54}Y_{0.19}Sn_{0.27}$ (δ)		$Pd_{0.64}Y_{0.09}Sn_{0.27}$ (ε)	
d [Å]	Intensity	*d* [Å]	Intensity	*d* [Å]	Intensity
4.176	m	4.55	w	3.06	w
2.544	s	2.457	vs	2.83	w
2.469	s	2.315	w	2.52	w
2.445	s	2.158	s	2.28	s
2.349	m	2.106	w	2.26	s
2.292	m	2.064	m	1.60	m
2.174	s	1.964	m		
2.044	s				
1.621	w				

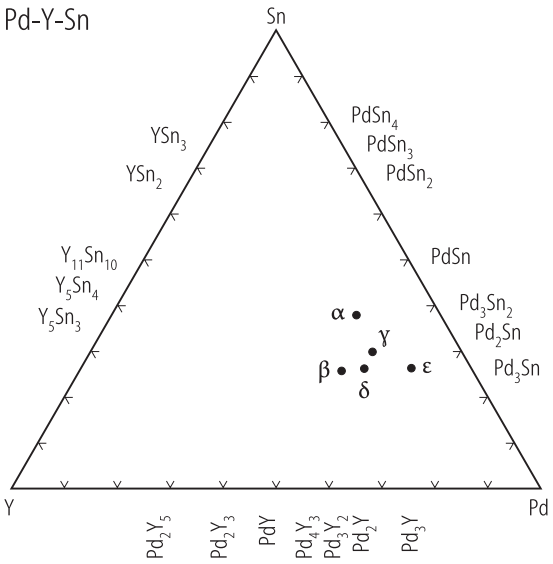

Fig. 36. Ternary phase diagram of the Pd–Y–Sn system. Of the new ternary compounds α, β, γ, δ and ε reported only the structure of the α and β phases could be determined. The α phase forms peritectically at 1228 K with a hexagonal structure with space group P6/mmm and lattice parameters a = 19.891 Å. Pd_2YSn, the β phase forms congruently at 1748 K, with the Heusler $L2_1$ structure [85J3].

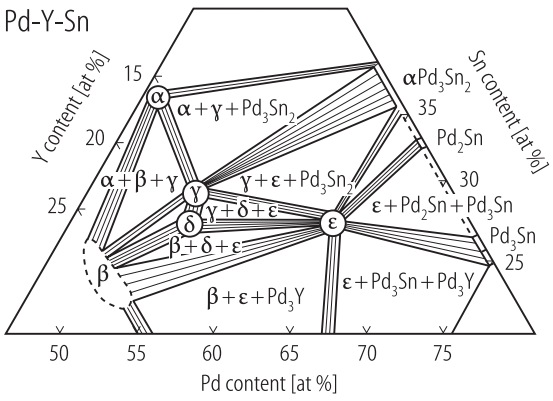

Fig. 37. Isothermal section of the partial Pd–Y–Sn system at 1075 K. The tie lines for the two-phase fields are schematic [85J3].

Fig. 38. Microprobe analysis in the two- and three-phase regions in Pd–Y–Sn [85J3].

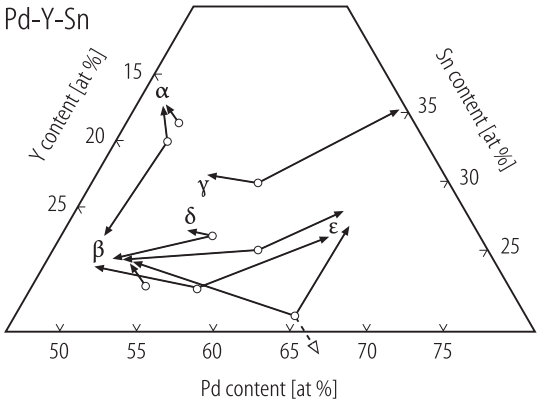

1.5.5.2.3 Kinematics of phase transition

The kinematics of the atomic ordering process were reviewed previously [88W1]. Further work has appeared on the Cu–Mn–Al system. As indicated in Table 10, the phase diagram is particularly complicated. Of particular interest is the simultaneous occurrence of two types of structural phase transition: the order-disorder transformations in the range of β phase and the decomposition of the β phase in the temperature range of its metastability.

The stability of metastable precipitates with the $L2_1$ structure has been investigated in Fe–Nb–Al up to 600 °C as a function of time.

The precipitation reaction has been studied in the Ni–Ti–Al system with the aim of improving the creep behaviour. Upon cooling, the alloys undergo a spinodal-ordering reaction.

Disorder trapping has been investigated in a rapid cooled Ni_2TiAl specimen. The alloy formed from the melt with the non-equilibrium B2 structure transforms to the $L2_1$ structure on cooling to room temperature.